Combustion and radiation modeling of laminar premixed flames using OpenFOAM: A numerical investigation of radiative heat transfer in the RADIADE project

Haider, Sajjad; Pang, Kar Mun; Ivarsson, Anders; Schramm, Jesper

Published in:
Papers, CIMAC Congress 2013

Publication date:
2013

Document Version
Publisher's PDF, also known as Version of record

CONSEIL INTERNATIONAL
DES MACHINES A COMBUSTION

INTERNATIONAL COUNCIL
ON COMBUSTION ENGINES

PAPER NO.: 274

Combustion and radiation modeling of laminar premixed flames using OpenFOAM: A numerical investigation of radiative heat transfer in the RADIADE project

Sajjad Haider, Technical University of Denmark, Denmark
Kar Mun Pang, Technical University of Denmark, Denmark
Anders Ivarsson, Technical University of Denmark, Denmark
Jesper Schramm, Technical University of Denmark, Denmark

Abstract: This paper presents the computational fluid dynamics modelling of a laminar premixed flame. A specific solver named 'rareLTSFoam' is developed using OpenFOAM ® code. The solver is used to simulate experimental stoichiometric and rich laminar premixed flames. The modelling is carried out for thermal flow and combusting flow cases. The results show that without including radiation modelling, the predicted flame temperature is higher than the measured values. P1 radiation Model is used with sub-models for absorption and emission coefficients. The model using constant values for the absorption and emission coefficients gave good agreement with measurements for the regions close to burner outlet. However, the weighted Sum of Gray Gas model (WSGGM) reasonably predicts the flame temperature as the flame height about the burner outlet increases.

INTRODUCTION

The combustion process in compression ignition (CI) engines is very complex in nature. Measurements [1] have shown that initially ignition occurs in rich premixed fuel air pockets formed by liquid fuel jet breakup and evaporation. The heat release from the ignition results in a diffusion flame at the jet periphery, and a rich premixed flame on the interface between incoming rich premixed fuel vapours and air and the hot combustion products. The multistage combustion process together with turbulence interaction and chemical kinetics has made it very challenging for the researchers to develop better numerical models. Investigation and prediction of soot formation and nitrogen oxides (NO_x) production requires better modeling tools and experimental analysis to be conducted. This in turn helps for developing future engine designs with higher efficiency and fewer emissions.

In CI engines, compared to spark ignition engines, the contribution of radiative mode of heat transfer is significant due to soot particles [2]. Radiation results in decreasing the temperature of the domain and increases heat transfer to the cylinder walls. As a result the influence of radiation on different in-cylinder phenomena such as NO_x formation etc. cannot be ignored. Currently, influence of heat radiation from gasses and particles is usually not or at least only in very simplified ways accounted for in state-of-the-art models of in-cylinder flow in combustion engines.

The RADIADE project is initiated at Section of Thermal Energy Section (TES-DTU) in collaboration with MAN Diesel and Turbo A/S as well as other collaborators. The aim of the RADIADE project is to enhance capabilities of computational models to understand the complex coupling between the radiant heat transfer, rate of combustion progress and formation of harmful products in combustion processes. The interest in radiation comes from the large dimensions of marine diesel engines, where radiation as a consequence is expected to be more influential on heat transfer than heat convection. The project involves detailed experimental measurements on different flames and developing models validated by the experimental measurements.

In the current work, the flame under consideration is a laminar premixed Ethylene (C_2H_4) flame investigated at TES-DTU [3]. The premixed flame has significant role for entire combustion process in CI engines because it links the evaporation process of fuel spray and the diffusion combustion [3]. The premixed flame temperature influences the temperature of diffusion flame via intermediate flame temperature, and also the decomposition of intermediate fuel to soot and H_2. Measurements [1] have shown that in diesel combustion the product gas of premixed flame acts as a fuel for the diffusion flame. At the pre-mixed flame front, the temperature of the rich fuel and air mixture is about 825 K [1] which makes the long chained alkanes unstable and crack to lighter hydrocarbons. Ethylene (C_2H_4) for premixed flame provides a simple substitution to the cracked diesel fuel because it has a C/H ratio of 0.5 which is close to the value of 0.56 for diesel [3].

One of the aims of RADIADE project is to develop models based on an open source Computational Fluid Dynamics (CFD) code. This provides flexibility and freedom in terms of code access and modification. In addition, the models/codes developed in this project will be shared with the scientific community for contributing in the development of improved computational tools. Open source CFD software OpenFOAM® includes several combustion solvers for different flame types using approaches such as partially stirred reactor (PaSR), Eddy Dissipation Concept (EDC) and flamelet models. Therefore, OpenFOAM® is employed to simulate the combustion and radiation processes in the laminar premixed Ethylene (C_2H_4) flame. This work is expected to serve as a prerequisite for the future numerical investigation of turbulence/chemistry interaction in diesel combustion in marine diesel engines.

For modelling the laminar premixed flame, in this work, a new solver is developed by modifying an existing solver, LTSReactingParcelFoam. Akin to reactingFoam which has been widely used in combustion simulations [4], LTSReactingParcelFoam is also applicable for laminar and turbulent reacting flow but it is a local time stepping solver for steady-state simulations. The modified version is henceforth addressed as radiationReactingLTSFoam (rareLTSFoam). This section first details the CFD transport equations and sub-models implemented in the current work,

with an emphasis on the modeling of combustion and radiation which is the main discussion here. It is then followed by the descriptions of chemical reaction schemes as well as mesh configuration and boundary condition settings. In the subsequent part, the local time stepping (LTS) solver which is used to reduce the computational runtime is depicted. Simulations results are then discussed and the conclusion is highlighted.

CFD MODEL FORMULATION

The transport equations for the simulation of compressible, reacting flow are solved here. These include the basic mass, momentum and enthalpy transport equations [5]. Apart from these, the species mass conversation and radiation transport equations are also considered in the calculation. The flow is laminar in the present test cases and hence no turbulent model is implemented. As such, the species transport equation is expressed in the following form,

$$\frac{\partial \overline{\rho} Y_i}{\partial t} + \nabla.\left(\overline{\rho}\vec{U}Y_i\right) = \nabla.\left(\mu \nabla Y_i\right) + \kappa\overline{RR_i} \qquad (1)$$

where, $\overline{\rho}$, Y_i, $\vec{U}$ and μ denote the density, mass fraction of *i-th* specie, velocity and dynamic viscosity, respectively. The second term on the right hand side of Equation (1) represents the source term. When turbulence is present, the turbulence/chemistry interaction is modeled based on the Chalmers' PaSR approach [6][7]. However, turbulent reaction does not exist in the cases presented in this work and the reactive volume fraction, κ in the PaSR model is automatically set to unity. The source term is hence purely contributed by the net production rate of species. The net production rate of species provided by the global chemical reaction, as detailed in the next sub-sections, is imported into their respective species transport equation.

Radiation Modelling

For an absorbing, emitting and scattering medium at position $\vec{r}$ and direction $\vec{S}$, the radiative transfer equation (RTE) [8] is given in as

$$\frac{dI(\vec{r},\vec{s})}{ds} + (\alpha+\sigma_s) I(\vec{r},\vec{s}) = \frac{\sigma_s}{4\pi}\int_{4\pi} I(\vec{r},\vec{s}') \, \Phi(\vec{s}-\vec{s}') \, d\Omega' + an^2\frac{\sigma T^4}{\pi} \qquad (2)$$

This equation describes the rate of change of radiation intensity at position $\vec{r}$ along the path ds and in the direction $\vec{s}$.

The P-1 radiation model is the lowest order case of the P-N model which provides an approximate solution of the integro-differential RTE (Equation 2) by transferring RTE into a set of simultaneous partial differential equations [9].

For a gray gas, the radiation flux, q_r [7] is given below as

$$q_r = -\Gamma \nabla G \qquad (3)$$

where G is the incident radiation and

$$\Gamma = \frac{-1}{\left(3(\alpha+\sigma_s) - C\sigma_s\right)} \qquad (4)$$

The transport equation for G is

$$\nabla.(\Gamma \nabla G) - \alpha G + 4\alpha n^2 \sigma T_g^{\,4} = S_G \qquad (5)$$

where n is the refractive index of the medium, T_g is the gas temperature and S_G is the user-defined radiation source. Combining Equations (3) and (5) give the expression for radiative heat flux,

$$-\nabla q_r = \alpha G - 4\alpha n^2 \sigma T_g^{\,4} \qquad (6)$$

Weighted Sum of Gray Gases Model

The weighted sum of Gray Gases Model (WSGGM) provides the total emissivity and absorptivity of a gas mixture as a sum of emissivities of fictitious gray gases weighted with a temperature dependent weighting factor [9].

$$\varepsilon = \sum_{i=0}^{I} a_{\varepsilon,i}(T_g)(1 - e^{-\alpha_i ps}) \qquad (7)$$

where α_i is the absorption coefficient of the *i*-th fictitious gray gas in the mixture, p is the sum of

the partial pressure of all participating gases and S is the beam path length. $a_{\varepsilon,i}$ is the emissivity weighting factor for the *i-th* fictitious gray gas and is approximated using a polynomial of order $J-1$ (Equation 8).

$$a_{\varepsilon,i}(T_g) = \sum_{j=1}^{J} b_{i,j} T_g^{\,j-1} \qquad (8)$$

α_i and $b_{i,j}$ are obtained by fitting Equation (7) to the data from the experimental measurements. For the current work, the WSGGM parameters are taken from [10].

Thermal Flow Model

Considering the fixed position and uniformity of the flame front just above the flame holder (Figure 1), it is reasonable to assume that at the outlet of flame holder the hot combustion products are coming out. As a first step, simulation of this thermal flow is conducted. Two cases of a stoichiometric and a rich flame are considered [3]. The details are given below as

Stoichiometric Flame: Equivalence ratio φ = 1, an inflow of gas with 0.81 m/s in the normal direction, T_g =1931 K and molar concentrations of $x_{CO_2} = 0.128,\ x_{CO} = 0.002,\ x_{H_2O} = 0.13,\ x_{H_2} = 0.0$ and the rest is N_2.

Rich Flame: Equivalence ratio φ = 2.15, an inflow of gas with 1 m/s in the normal direction, T_g =1829 K and molar concentrations of $x_{CO_2} = 0.021,\ x_{CO} = 0.194,\ \ x_{H_2O} = 0.065,\ x_{H_2} = 0.151$ and the rest is N_2. No soot modeling is included.

Combusting Flow Model

In this work, for combusting flow model, the combustion simulation is conducted only for rich flame case. The 'cold boundary condition' is a known problem in laminar, premixed flame simulations [5]. In order to address this problem, the initial mixture temperature at premixed charge inlet is set at 1500 K such that it is sufficiently high to allow combustion to occur. The inlet temperature is then ramped down gradually over a specified period of time to the actual mixture temperature of 303 K. This is achieved by applying the time-varying boundary condition as listed in Table 1. The timespan is selected such that the flame is well established and the combustion sustains by itself even the inlet temperature is low. Table 1 summarizes the *OpenFOAM* boundary conditions used in the simulations for each variable while Table 2 details the species mass fraction and inlet velocity used in the rich flame case.

Table 1: Boundary conditions implemented in the current simulations.

	Premixed charge inlet	Helium co-flow inlet	Outlet	Wall
Pressure [Pa]	zeroGradient	zeroGradient	totalPressure	zeroGradient
Temperature [K]	timeVarying	fixedValue	fixedValue	fixedValue
Velocity [m/s]	fixedValue	fixedValue	fluxCorrected Velocity	fixedValue
G [kg/m^3]	Marshak	Marshak	Marshak	Marshak
Yspecies	fixedValue	fixedValue	inletOutlet	zeroGradient

Table 2: Species mass fraction and velocity used in the rich flame case.

	Premixed charge inlet	He co-flow inlet
Velocity [m/s]	(0.135, 0, 0)	(0.048, 0, 0)
C_2H_4	0.1282	0
O_2	0.2031	0
N_2	0.6687	0
He	0	1
Yspecies	0	0

Chemical reaction scheme

Chemical equilibrium is reached here and the flame temperatures near burner surface are measurable from the experiments. With this feature and information, the *Gaseq* software is exploited to calculate the resulting composition in order to construct a simple, global reaction for the rich flame [11]. The reason to customize the global, irreversible reactions in this work is twofold. First of all, the implementation of such simplified chemical

scheme assists in minimizing the computational runtime. Meanwhile, the composition of the combustion products i.e. CO_2, H_2O, CO and H_2 is accurately replicated. The radiative properties of the former two compounds are the decisive factor in accurate modeling the radiative heat transfer and hence a good prediction of the composition is important.

A global irreversible chemical reaction as shown in the form of equation (9) is then constructed based on their respective composition detail for the rich flame. The number of moles of each species calculated by the *Gaseq* software and the Arrhenius parameters used in the current simulations are summarized in Table 3.

$$uC_2H_4{}^{a} + vO_2{}^{b} = wCO_2 + xCO + yH_2O + zH_2 \quad (9)$$

Table 3: Details for the global reaction used in rich flame simulation.

Mole	Rich flame
U	*5*
V	*7*
W	*9*
X	*1*
Y	*7*
Z	*3*
Arrhenius Reaction Parameters	
Pre-exponential factor, *A*	7.14174
Temperature dependence, *β*	0
Activation temperature, T_a	15095.7
Fuel reaction order, *a*	0.1
Oxidizer reaction order, *b*	1.65

A, *β* and T_a are the pre-exponential factor, temperature dependence and activation temperature, respectively. These values as well as the reaction order values of both fuel and oxidizer are adopted from the single step reaction developed by [12]. It is however, observed that the laminar flame speed and hence the heat loss to the burner surface are not predicted correctly by using the default Arrhenius parameters. This is indicated by the maximum flame temperature measured near the burner surface at the height of 10mm. An accurate prediction of this temperature is crucial for the subsequent radiation modeling. The *A* value is therefore artificially adjusted in order to replicate the experimental temperatures. The *A* value of the global reaction for the rich flame is reduced to replicate a flame lift-off. The flame lift-off in the rich flame test case leads to a negligible heat loss to the burner surface. As such, the maximum flame temperature is increased. As for the chemistry solver, Semi-implicit Bulirsch-Stoer (SIBS) Ordinary Differentiate Equation (ODE) solver is used where 'initial chemical time step' and '*eps'* scale are set at 1×10^{-7} and 5×10^{-4}, respectively. This configuration is found to give both accurate results and system stability. Also, the implementation of this ODE solver reduces the computational runtime as compared to that of the Runge-Kutta solver.

Mesh configuration and boundary conditions

An illustration of the experimental flame chamber and model of fluid domain is given in Figure (1) [3]. This domain is used to represent a section of the combustion chamber where the radiative heat loss of the helium-stabilized, laminar premixed flame was experimentally investigated.

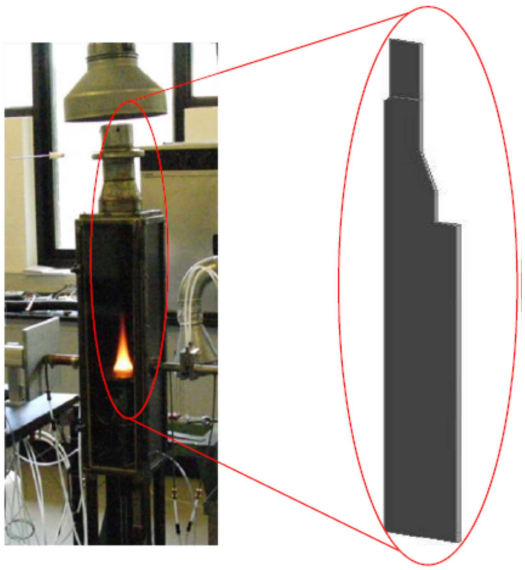

Figure 1: Experimental flame chamber with illustration of computational model domain.

Figure (2) shows the 4-degree sector computational grid, mirrored along the burner axis for better comparability. The mesh is generated using the *blockMesh* utility in OpenFOAM software. As

illustrated, the grid accounted for two inlets. The premixed charge of ethylene fuel and air enters the domain through the inlet at the center. On the other hand, helium gas flows into the domain at a velocity of 0.048 m/s. The domain also accounted for an internal wall such that the helium gas can be trapped to stabilize the flame. This corresponds to the experiment setup [3]. Apart from these, an outlet is located at the top of the computational domain where ambient condition is used. The remaining areas are defined as wall and all the wall temperatures, including that of the internal wall are fixed at 450 K [3].

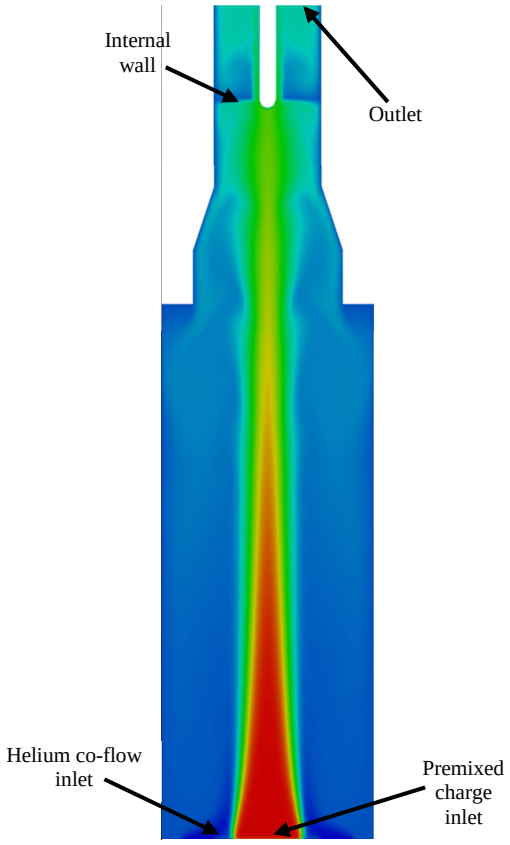

Figure 2: Computational domain used in the laminar, premixed flame simulations

Local Time Stepping (LTS) Solver

The *reactingFoam* solver utilizes Pressure Implicit with Splitting of Operators (PISO) algorithm which needs to be stabilized by using an extremely low maximum *Courant–Friedrichs–Lewy* (*CFL*) number, particularly in reacting flow cases [4]. The *CFL* number in one-dimensional case is defined as

$$CFL = \frac{u\Delta t}{\Delta x} \leq CFL_{\max} \qquad (10)$$

where u and Δx denote the local velocity and length interval of the computational cell, respectively. Δt on the other hand, refers to the global time step. Referring to Equation (10), the global time step is adjusted at each iteration to fulfill the *CFL* condition and the same global time step is used for all the cells throughout the computational grid [13]. In this approach, the smallest cell with the highest velocity leads to the need of a small time step and consequently, the overall computational runtime becomes long. Although larger cells with lower velocity could be driven with much larger time steps, they were prohibited.

In order to address this limitation, the LTS approach [14] is introduced to maximize the individual time step for each cell according to the local *CFL* number [15][16]. In the current simulations, the maximum *CFL* number is set at 0.5. No significant improvement in result accuracy is observed when a lower *CFL* number is implemented but a higher number of iterations is required to obtain the steady-state solution. On the other hand, a higher *CFL* number produces a much higher mass continuity error which is not desired. The solver then processes the time step fields by smoothing the variation in time step across the domain to avoid abrupt transitions caused by sudden changes in time step. *'coeff$_S$'* is the smoothing coefficient for the reciprocal of the time step. A low smoothing coefficient value of 0.1 is set to smooth the local time steps in all the neighbored cells and this value is retained throughout the simulation. In parallel to this, α_{Temp} is also designated to limit the change of the temperature. A value of 0.05 is retained in all the simulation such that the maximum increment of the temperature is within 5 % of the previous value. These values are selected to strike a balance between a practical computational runtime and system instability. For example, implementation of a high value of α_{Temp} leads to the rapid change of the predicted temperature and the simulation crashes as the temperature increases beyond the upper limit given by the JANAF thermochemical table.

RESULTS

For each thermal flow case, the simulations are carried out first without including any radiation modeling. Then the radiation modeling is included by using constant values of absorption/emission coefficients and WSGGM. The results are shown in Figures (3) and (4) for the stoichiometric and rich flame case respectively. The results show that, in absence of radiation model, the simulation predicts higher temperatures in the flame core and other measuring positions above the burner. Radiation

model using constant values of absorption/emission coefficients gives good prediction of the flame core temperature very close to the burner outlet. However, at increased heights above the burner surface, the model gives higher temperature values compared to the measurements. The WSGGM gives a lower flame core temperature but gives reasonable results at regions 90 mm and above. The flame temperature drop profile shape, along the height above burner, is also predicted reasonably well. This indicates that using an improved absorption/emission model can give promising simulation results.

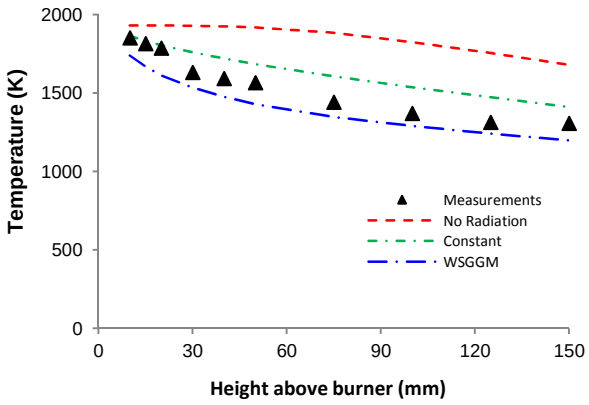

Figure 3: Stoichiometric flame thermal flow case

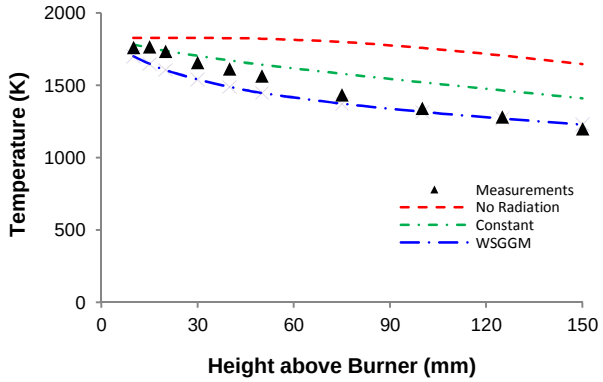

Figure 4: Rich flame thermal flow case

Contours of gas mixture temperature (mirrored along burner axis) in rich flame case are shown in the Figure (5b-1-2-3) for different thermal flow models. The contours shown are up to a height of 150 mm above the burner, same as for the picture of the experimental flame (Figure 5a) with measured values of temperature. From Figure (4) and (5b), it can be observed that the temperature contours in the experimental flame may be similar to Figure (5b-2) in the regions close burner outlet and to Figure (5b-3) in the regions 75 mm and higher, above the burner outlet.

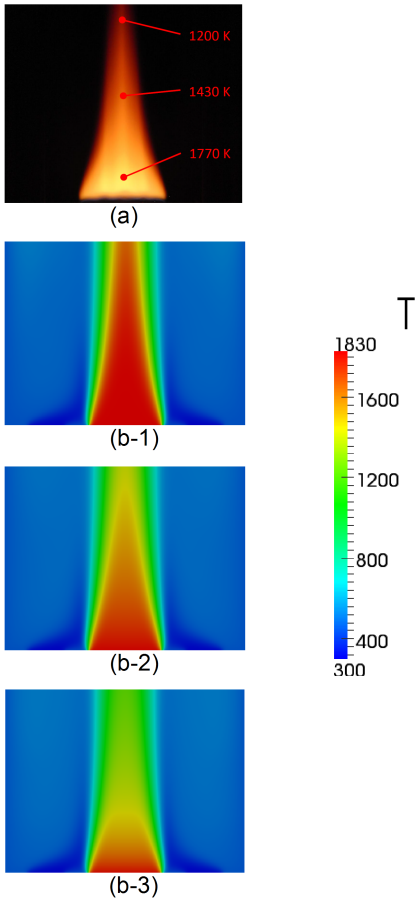

Figure 5: (a) picture of Helium Stabilized Rich flame [10]. (b) Contour of Flame Temperature distribution [K]: (b-1) No Radiation Modelling. (b-2) Constant Absorption/Emission Coefficient Model. (b-3) WSGGM

For the combusting flow model, the radiation model used is with constant absorption/emission coefficients. The temperature profile is shown in Figure (6).

The results indicate that the constant values of absorption/emission coefficients used give a good approximation of the experimental flame properties. Thus improvement and development of a better absorption/emission model is one of the main tasks in the future work.

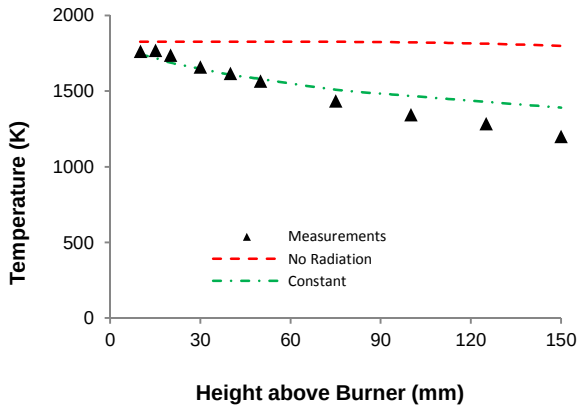

Figure 6: Rich Flame Combustion Case

CONCLUSIONS

In this research work, a numerical solver is developed to analyze the combustion characteristics of premixed flame and effect of including the radiation modelling on the performance of the model. The simulation results show that the developed solver can be used to model laminar premixed flames and also provides the option for including radiation modeling. The results from thermal flow cases indicate that radiation modeling has a significant effect on the prediction of flame temperature. In terms of predictive accuracy, the model using constant absorption and emission coefficients show better agreement at measured positions close to burner exit whereas the WSGGM gives a better prediction along the flame height. Besides using more advanced and computationally expensive radiation models than P1, the absorption and emission coefficient modelling for the gas mixture is also important. This requires the implementation of different modelling approaches in the current solver for the absorption and emission coefficients and also to use improved/recent WSGGM models than the one used in this work.

NOMENCLATURE

$\vec{s}'$	scattering direction vector
s	path Length
α	absorption coefficient
n	refractive index
σ_s	scattering coefficient
σ	Stefan-Boltzmann constant
I	radiation intensity
T	local temperature
Φ	phase function

Abbrevations

CFD	Computational Fluid Dyamics
CI	Compression Ignition
EDC	Eddy Dissipation Concept
WSGGM	Weighted Sum of Gray Gases Model
LTS	Local Time Stepping
PISO	Pressure Implicit with Splitting of Operators
SIBS	Semi-implicit Bulirsch-Stoer
ODE	Ordinary Differentiate Equation
CFL	*Courant*–Friedrichs–Lewy
PaSR	Partially Stirred Reactor

ACKNOWLEDGEMENTS

The authors acknowledge Strategic Research Council Denmark and MAN Diesel & Turbo A/S for funding the RADIADE project. We are also grateful to Domink Christ from WIKKI Ltd. UK for the OpenFOAM code for Weighted Sum of Gray Gases Model.

BIBLIOGRAPHY

[1] Flynn P.F., Durrett R.P., Hunter G.L., Loye A.Z., Akinyemi O.C., Dec J.E. and Westbrook C.K., Diesel Combustion: An Integrated View Combining Laser Diagnostics, Chemical Kinetics and Empirical Validation, SAE Technical Paper Series 19999-01-0509(1999).

[2] Sazhina E.M., Sazhin S.S., Heikal M.R. and Bardsley M.E.A, The P-1 Model for Thermal Radiation Transfer: Application to Numerical Modelling of Combustion Processes in Diesel engines. 16th IMACS World Congress 2000.

[3] Ivarsson A. “Modeling of heat release and emissions from droplet combustion of multi

component fuels in compression ignition engines" Ph.D. Thesis, Technical University of Denmark, 2009.

[4] Marzouk O. A., and Huckaby E. D. "A comparative study of eight finite-rate chemistry kinetics for CO/H_2 combustion" Engineering Applications of Computational Fluid Mechanics, Vol. 4, pp. 331-356 (2010).

[5] Poinsot T. J., and Veynante, D. "Theoretical and Numerical Combustion" R. T. Edwards Inc., (2001).

[6] Chomiak J., and Karlsson A. "Flame Liftoff in Diesel Sprays" Proceedings of the Combustion Institute, Vol. 26, pp. 2557-2564(1996).

[7] Golovitchev V. I., Nordin N., Jarnicki R., and Chomiak J. "3-D diesel spray simulations using a new detailed chemistry turbulent combustion model" SAE Paper 2001-01-1891 (2001).

[8] ANSYS FLUENT® Manual.

[9] Modest F. M. Radiative Heat Transfer, Second Edition, Academic Press (2003).

[10] Smith T.F., Shen Z.F., Friedman J.N., Evaluation of Coefficients for the Weighted Sum of Gray Gases Model, J. Heat Transfer, Vol 104(4), pp 602-608 (1982).

[11] Morley C., gaseq version 0.79, available at <*http://www.gaseq.co.uk/*> (accessed on 19 july 2012).

[12] Westbrook C. K., and Dryer F. L. "Simplified Reaction Mechanism for the Oxidation of Hydrocarbon Fuels in Flames" combustion science and technology, vol. 27, pp 31-43(1981).

[13] Courant R., Freidrichs K., and Lewy H. "On The Partial Difference Equations Of Mathematical Physics" IBM Journal of Research and Development, Vol. 11, pp. 215–234(1967).

[14] Arnone A., Liou M.S. and Povinelli l. A. "Multigrid Time-Accurate Intergration Of Navier Stokes Equations" NASA Technical Memorandum 106373, Icomp 93-97(1993).

[15] OpenFOAM The Foundation, Available at <*http://www.openfoam.org/version2.0.0/steady-vof.php*> (Accessed on 17 March 2012).

[16] Becker M., "Dhcaeltsthermoparcelsolver" Dhcae Tools, Available at <*http://www.dhcae-tools.com/images/dhcaeltsthermoparcelsolver.pdf*> (Accessed On 19 July 2012).